

Early warning signals for desynchronization in periodically forced systems

Pablo Rodríguez-Sánchez

Egbert H. Van Nes

Marten Scheffer

2020-02-29

Abstract

Conditions such as insomnia, cardiac arrhythmia and jet-lag share a common feature: they are all related to the ability of biological systems to synchronize with the day-night cycle. When organisms lose resilience, this ability of synchronizing can become weaker till they eventually become desynchronized in a state of malfunctioning or sickness. It would be useful to measure this loss of resilience before the full desynchronization takes place. Several dynamical indicators of resilience (DIORs) have been proposed to account for the loss of resilience of a dynamical system. The performance of these indicators depends on the underlying mechanism of the critical transition, usually a saddle-node bifurcation. Before such bifurcation the recovery rate from perturbations of the system becomes slower, a mechanism known as critical slowing down. Here we show that, for a wide class of biological systems, desynchronization happens through another bifurcation, namely the saddle-node of cycles, for which critical slowing down cannot be directly detected. Such a bifurcation represents a system transitioning from synchronized (phase locked) to a desynchronized state, or vice versa. We show that after an appropriate transformation we can also detect this bifurcation using dynamical indicators of resilience. We test this method with data generated by models of sleep-wake cycles.

1 Introduction

The phenomenon of endogenous circadian rhythms, first observed by the French polymath Jean-Jacques d’Ortous de Mairan in 1729 (d’Ortous de Mairan [1729]), has transcended science to become part of the popular culture, often referred to as *the inner clock*. The evolutionary convenience of synchronizing such *inner clocks* with the external cues, usually provided by regular astronomical events such as day-night periods and seasons, is well established (Foster and Kreitzman [2017]). Synchronization, thus, proves useful for living systems and a difficulty to synchronize (and sometimes also to desynchronize) can be an indicator of sickness or malfunctioning. Some synchronization-related conditions include insomnia, jet-lag, arrhythmia or epilepsy (Glass [2001]).

The transition from a synchronized to a desynchronized regime is discontinuous. The system is either synchronized or not. Therefore it could be that synchronization is a special kind of critical transition (Scheffer [2009]). This is relevant as there have been developed ways to foresee whether at critical transition is likely to occur (Scheffer et al. [2009]). These dynamic indicators of resilience (DIORs) are based on the phenomenon of “critical slowing down” (Wissel [1984], Van Nes and Scheffer [2007]). According to this theory, the recovery rate from perturbations decreases if systems are close to a critical transition. In time series we can measure critical slowing down using different indicators, such as increased autocorrelation and variance (Dakos et al. [2012]).

In the present work we illustrate with simple models that some transitions from synchronized to desynchronized states indeed can be related to a special kind of critical transition, namely a saddle-node bifurcation of cycles. We show that after an appropriate transformation of the data, we can still use critical-slowness indicators to see if one of these transitions is likely to happen.

2 Methods

2.1 Case study model

Our goal is to develop generic indicators for the risk of desynchronization of biological cycles such as the sleep-wake cycle. To understand the properties of this system, we analyze a generic model of such periodically forced cyclic systems. This minimal model consists of two oscillators: a master (representing the external forcing, for instance of a diurnal rhythm) and a slave (representing the organism's state, for instance its sleep/awake status). We represent each oscillator by its most basic feature: phase (θ_\odot for the master and θ for the slave). The master's frequency is constant (i.e. the phase grows steadily from 0 to 2π in 24 h), and it is not affected by the slave's dynamics. The slave's dynamics are more complex: in the absence of coupling it has a natural frequency, and an increasing tendency to synchronize with the master if the coupling gets more intense. These features are captured by model (1).

$$\begin{cases} \frac{d\theta}{dt} &= \omega - k \cdot f(\theta - \theta_\odot) \\ \frac{d\theta_\odot}{dt} &= \omega_\odot \end{cases} \quad (1)$$

In model (1) each oscillator shows a natural frequency (ω and ω_\odot). The first oscillator shows a tendency to slow-down if θ is ahead of θ_\odot , and to speed-up otherwise. The function f measures the difference between θ and θ_\odot . Note that f has to be a periodic function (in the sense of $f(x + 2\pi) = f(x)$). This is a consequence of the cyclic nature of phases: by definition phases θ and $\theta + 2\pi$ represent the same point in a cycle, and thus, the same physical reality. In most applications f is also continuous and smooth. The strength of the coupling is given by the positive constant parameter k . If the coupling is not strong enough (relative to the difference in natural frequencies), synchronization doesn't happen.

The system (1) becomes simpler (and even analytically tractable) if we use the phase difference $\phi(t) \equiv \theta(t) - \theta_\odot(t)$ as a new state variable. With this change of state variable, the system takes the form (2), where, for convenience, we made $\Omega \equiv \omega - \omega_\odot$.

$$\frac{d\phi}{dt} = \Omega - k \cdot f(\phi) \quad (2)$$

For the sake of clarity, we will use $f(\phi) = \sin(\phi)$ in the rest of this work. As we discuss in the online appendix, we can do this without loss of generality. With this choice, our model becomes a simple subcase of the classical Kuramoto model (see Kuramoto [1975], Strogatz [2000]). Equating (2) to zero, the stable and unstable equilibria of our system are easily found to be $\phi_s^* = \Delta$ and $\phi_u^* = \pi - \Delta$, where $\Delta \equiv \arcsin \frac{\Omega}{k}$. It is important to note that, for those equilibria to exist, condition (3) should be satisfied. Intuitively, this means that our system can only synchronize cycles whose difference in natural frequencies (Ω) have at most the same order of magnitude as the coupling term (k).

$$\left| \frac{\Omega}{k} \right| \leq 1 \quad (3)$$

When condition (3) is satisfied, the system (2) tends naturally to the stable solution. In this case, the phase difference ϕ is constant, so both oscillators have the same frequency (ω_\odot) and are thus synchronized. If, on the contrary, condition (3) is not satisfied, the phase difference ϕ never stabilizes and consequently synchronization is not possible.

But, what happens at the border between both cases, that is, when Ω/k approaches 1? In such a situation, the stable and unstable solutions collide and annihilate each other at $\phi^* = \frac{\pi}{2}$ (see first row of panel 1). This mechanism of losing stability is known as a saddle-node bifurcation (Kuznetsov [1998], Strogatz [1994]). For an extensive discussion about the choice of this system, please refer to the appendix.

We'll take advantage of the periodicity of our system by plotting its trajectories over a $2\pi \times 2\pi$ square with periodic boundary conditions (or, equivalently, on the surface of a torus). When the phase hits any border, it reappears at the opposite side (just like in old-school video games such as *Pac Man* or *Asteroids*). In figure 1 we see three different configurations of such a system. As our parameter approaches the saddle-node bifurcation, both the stable and unstable cycles get closer. When we introduce additive

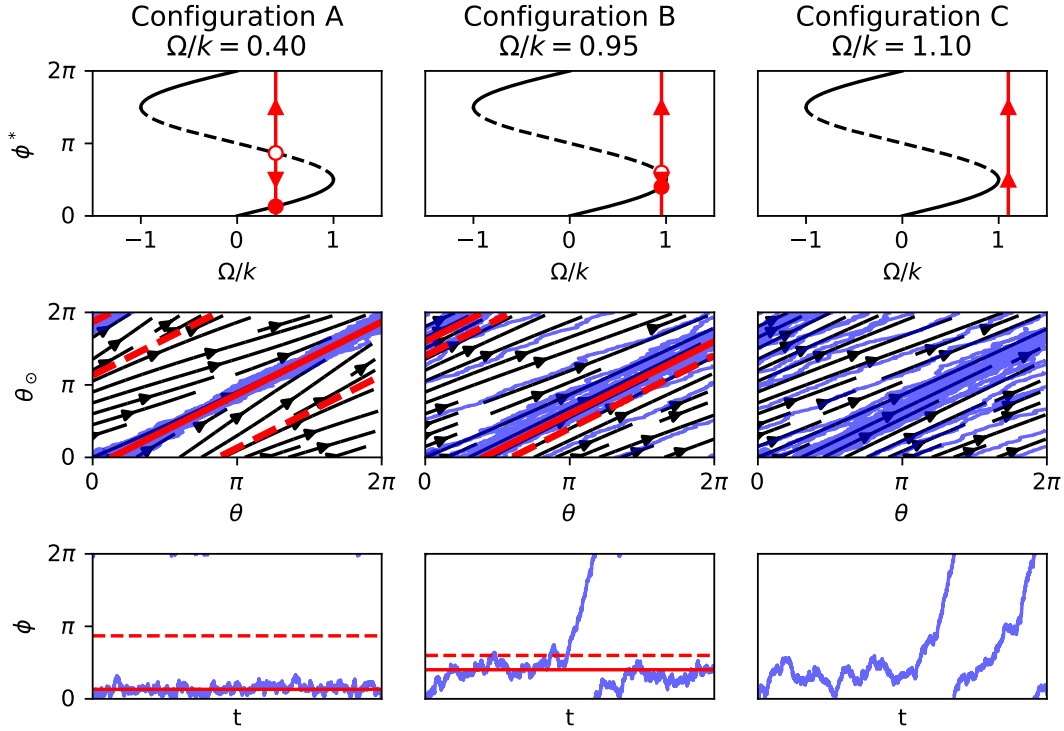


Figure 1: Each of the columns corresponds to a different configuration for system (1), identified by the value of the bifurcation parameter Ω/k , which represents the synchronization capacity. From left to right, each column represents less coupling strength. Each of the rows corresponds to a different representation of the dynamics. In the first row we see the bifurcation diagram of the phase difference (ϕ). The red arrows in the first row represent the flow on the line. In the second and third rows, the continuous red line represents the stable branch, and the dotted one the unstable branch. Saddle-node bifurcations happen at $\frac{\Omega}{k} = \pm 1$. If $|\frac{\Omega}{k}| > 1$ the system has no equilibrium solution and, thus, represents a desynchronized system. In both the second and third rows, the continuous red lines represent the stable cycle, and the dashed line, the unstable one. We plot in blue one simulated trajectory, under the influence of stochastic noise (modelled as a Wiener process with a variance of $\sigma^2 = 0.04$). The second row uses (θ, θ_\odot) as coordinates (phase space) and the third row uses (t, ϕ) coordinates (time series). Notice that in the second column, even if $\frac{\Omega}{k} < 1$, a noise induced transition may happen due to the proximity of the stable and unstable cycles.

noise to the dynamics, transitions can happen before the bifurcation is reached if the noise is strong enough to make the state jump the gap between both cycles (figure 1, column B). Note that due to the periodic boundaries the system is only momentarily desynchronized as it “collapses” back to the synchronized dynamics.

2.2 How to extract phase differences from data?

From the previous subsection it should be clear that synchronization is related to a fold bifurcation that occurs in the phase difference of the internal clock of a system respective to that of the forcing. This phase difference is usually not directly measurable. Instead, experimental data of periodic phenomena usually gives us indirect information about the phase. The angle of the Sun respective to the local meridian, the height of the tide or even the subjective feeling of sleepiness or hunger along the day are obviously affected by the phase of the cycle under study (see figure 2). But, can we use these indirect measurements to robustly infer the phase?

In order to answer this question, we will translate the ideas illustrated in the previous paragraph and figure 2 to mathematical language. Particularly, we’ll assume, as a working hypothesis, that there is a certain functional relationship M between the phase of the cycle $\theta(t)$ and our observations $y(t)$ (equation (4)). Due to the periodic nature of our problem, we expect M to have a period of 2π .

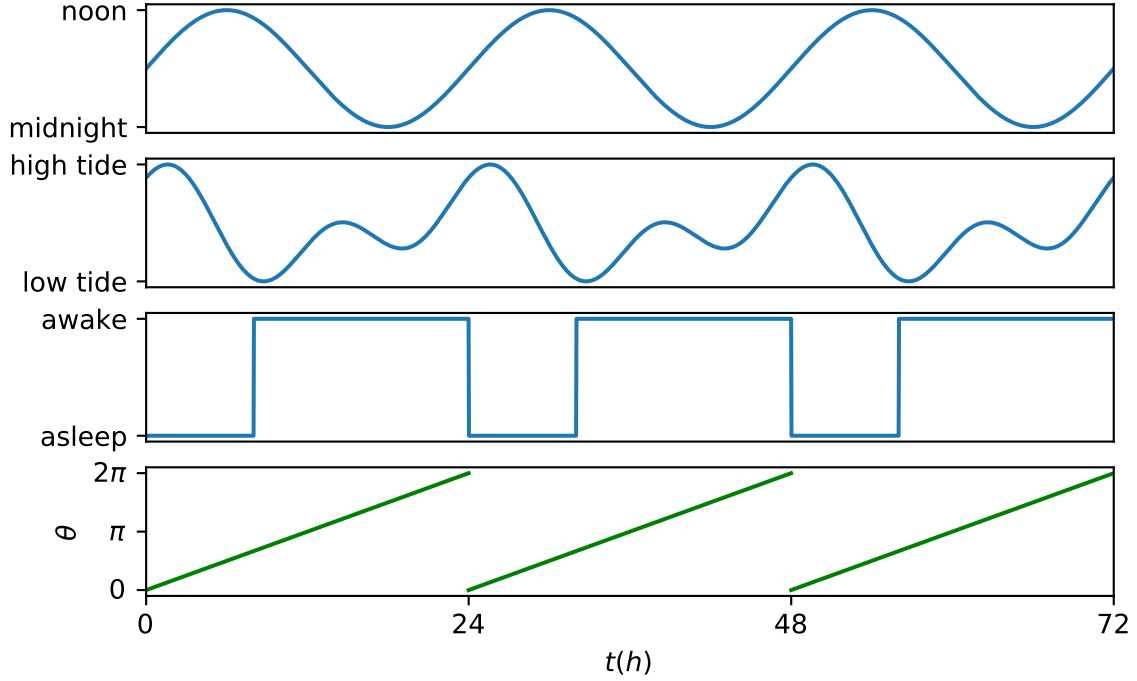


Figure 2: The first row shows the Sun’s angular height from a local horizon. Second row represents the height of the tide. Third row shows a sleep wake cycle of a healthy individual. The fourth and last row shows a common phase for the three above-mentioned phenomena (thus, the time series in all rows can be expressed in the form given in equation (5)). All series have been plotted for three whole periods.

$$y(t) = M[\theta(t)] \quad (4)$$

We define a reference cycle $y^{ref}(t)$ based in our knowledge about the system under study. For instance, if we are studying sleep cycles and $y(t)$ represents the asleep state, a reasonable choice for $y^{ref}(t)$ could be $y^{ref}(t) = 0$ (awake) if t is between 8 and 24 h, and 1 (asleep) otherwise. Such a function represents the idealized sleeping cycle of a healthy individual. We assume the reference cycle to be the result of applying the unknown function M to the phase of the external forcing θ_\odot (equation (5)).

$$y^{ref}(t) = M[\theta_\odot(t)] \quad (5)$$

If our system is either synchronized or subject to slow variations in its external conditions, we can consider the phase difference ($\phi(t) \equiv \theta(t) - \theta_\odot(t)$) approximately constant over a given time span $[t_a, t_b]$. It can be shown (see appendix section A.1) that under this circumstances we can expect that $y(t)$ is just shifted in time relative to $y^{ref}(t)$ by a certain time delay λ (equation (6)).

$$y(t) = y^{ref}(t + \lambda) \quad (6)$$

We find the time delay λ that best fits our data by minimizing the sum of squares between the time-shifted reference cycle and our measurements (see figure 3 and equation (7)). This time delay λ_{min} is proportional to the phase difference. In section A.1 of the appendix, we show that, specifically, $\phi = \omega_\odot \lambda_{min}$.

$$D^2(\lambda) = \sum_{i=a}^b (y_i - y^{ref}(t_i + \lambda))^2 \quad (7)$$

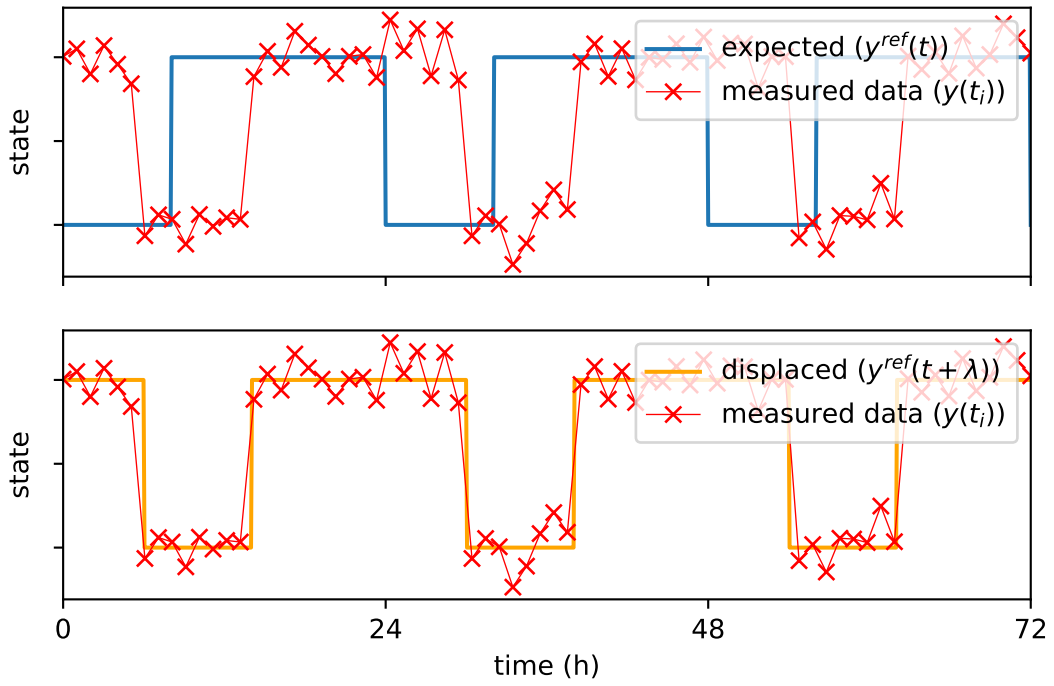


Figure 3: In both panels the red crosses represent the hypothetical activity of a human being experiencing a jet lag, measured every 60 minutes during 3 days. In the upper row we see the expected daily activity in blue (no activity while sleeping between 0 and 8 hours, and activity the rest of the day). In the lower row we see, in orange, the expected daily activity, but now displaced 6h in the time axis. This displacement provides the best fit for the data, and is calculated by minimizing the function $D^2(\lambda)$ given in equation (7).

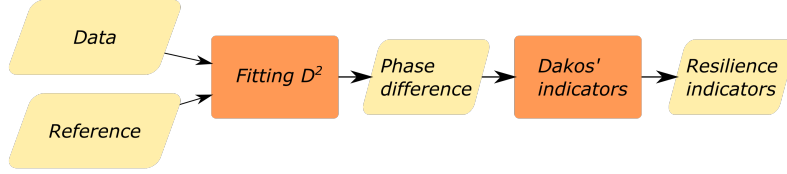


Figure 4: Schematic outline of our method.

Applying the method described above to different time windows allows us to use data to estimate a time series of the phase differences ($\phi(t_j)$) even if the precise analytical form of M is unknown (see first row in figure 5 and second row in figure 6). See appendix section A.1 for details.

2.3 Resilience indicators

Saddle-node bifurcations are often preceded by the phenomenon of critical slowing down (Scheffer et al. [2009]). Such a phenomenon can be directly observed in the time series even if the underlying dynamics are unknown. In the present manuscript we used the above-mentioned minimization algorithm along a moving window of typically 1-day width to extract the phase difference. Then, we applied the methods proposed by Dakos (Dakos et al. [2012]) to analyze this time series. Particularly, we first detrended the time series by simply subtracting the average value over non-intersecting windows of 1 day length. Afterwards, we calculated the standard deviation and autocorrelation of the residuals, using a rolling window with a length around 25-50% of the original time series' length. The optimal parameters (window length, autocorrelation lag, etc.) depend on the time scale and characteristics of the data under study. For more details about this method, see Dakos et al. [2012]. For an extended discussion about the limitations of these methods, see Dakos et al. [2015].

Figure 4 summarizes all the steps, inputs and outputs of our method.

2.4 Model-generated time series

We tested our method with two model-generated time series.

The first time series was generated with the help of the sleep-wake model of Strogatz (Strogatz [1987]). We configured the system so the time series represents the sleep-wake dynamics of an individual that is becoming progressively more prone to insomnia. The insomnia effect was simulated by allowing the coupling term k to linearly decrease to zero along a period of 135 days. This makes the individual's inner clock progressively less capable of coupling with the day-night cycle, and eventually completely unable to do so. Strogatz's model (Strogatz [1987]) can be understood as a Kuramoto oscillator followed by a postprocessing function M that transforms the inner clock's phase θ into a sleep-wake time series. Particularly, $M(\theta)$ returns 1 (awake) if the inner clock's phase θ is between $2\pi/3$ and 2π radians (corresponding to 8 and 24 hours in the inner clock), and 0 otherwise (asleep). We used the generated time series to estimate the phase difference. As this model contains an explicit phase, we can use it as a control, and compare it with our estimated phase as a verification of our method for extracting phases from data (see first row of figure 5).

To show the generality of our method, we applied it to a second time series generated with a more realistic model, the Phillips-Robinson model (Phillips and Robinson [2007]). The Phillips-Robinson model is a deterministic sleep-wake model based on neurological considerations, and it doesn't contain an explicit phase. It describes the time evolution of three state variables: V_v the activity of the ventrolateral preoptic area (prompting the body to stay asleep), V_m the activity of the mono aminergic group (prompting the body to stay awake) and H the homeostatic pressure (an auxiliary variable that quantifies the need for sleep). The dynamics of the model are given by the equations (8), where $F(V)$ is a saturation function given by (9) and $C(t)$ (defined in equation (10)) is a time-dependent external forcing, representing the astronomical light/dark cycle. The remaining elements in equation (8), including the influence of the acetylcholine group (V_{ao}), are just constants. The parameters used are the same as in (Phillips and Robinson [2007]); see section A.3 in the online appendix. Additionally, this appendix section provides a graphical representation of the relationships in equation (8).

$$\begin{cases} \tau_v \frac{dV_v}{dt} &= -V_v & -\nu_{vm}S(V_m) & +\nu_{vh}H & -\nu_{vc}C(t) \\ \tau_m \frac{dV_m}{dt} &= -V_m & -\nu_{mv}S(V_v) & & +\nu_{ma}S(V_{a0}) \\ \chi \frac{dH}{dt} &= -H & +\mu S(V_m) & & \end{cases} \quad (8)$$

$$S(V) = \frac{Q_{max}}{1 + e^{-\frac{V-\theta}{\sigma}}} \quad (9)$$

$$C(t) = \frac{1}{2} (1 + \cos(\omega t + \alpha)) \quad (10)$$

Once again, we simulated an individual whose sleep quality is slowly deteriorating. We achieved this effect by allowing the coupling parameter ν_{vc} to decrease linearly from its normal value of 6.3 mV to 0 mV along a period of three months. By doing this, the ability of the subject to synchronize his internal clock with the external time cues slowly disappears. The first episode of insomnia/desynchronization happens on the 83rd day (see first row in figure 6).

In order to simulate the fluctuations expected in any biological system we added noise to the integration of both our time series. In particular, we modeled our systems as Wiener processes. The deterministic terms have been described in the previous paragraphs. The stochastic terms ($dW = \sigma dt$) for Strogatz's model were set to $\sigma = 0.05$ for the inner clock's phase, and to 0 for the driver. For the Phillips-Robinson model, the stochastic term was set to $\sigma = 1$ for the states V_v and V_m , and 0 for H . The integration was performed numerically with the Python package *sdeint*.

3 Application

We applied the minimization algorithm described in the methods section to the sleep-awake time series generated with Strogatz's model (see methods). As a reference of a healthy sleep-wake cycle, we used a simple assumption: a healthy individual is awake between 8 in the morning and 24 at night, and asleep otherwise. We managed to reconstruct correctly the phase difference. The reconstructed phase difference shows the classical signs of slowing down (namely, increase in standard deviation and autocorrelation) when the system is approaching the bifurcation (see figure 5).

Our method was also applied with success to the time series generated with the Phillips-Robinson model (equation (8)). We focused our attention only in the time series corresponding to the state variable H . We used the time series corresponding to day 1 as a reference to estimate the phase difference. Particularly, we built $y^{ref}(t)$ as a quadratic interpolator of the measurements corresponding to the first day. As we can see in figure 6, the first episode of insomnia (83rd day) is preceded by an increase in both standard deviation and autocorrelation of the estimated phase difference.

4 Discussion

In the current work we presented a way of deriving dynamic indicators of resilience (DIORs) for systems transitioning from synchronized to desynchronized states through the family of bifurcations known as saddle-node of cycles. Our method is designed for time series, and doesn't require detailed knowledge of the deterministic dynamics of the system. This makes it particularly suitable for biological systems where a loss of synchronization may have an undesired effect (such as insomnia or arrhythmia (Glass [2001])) or may be an indicator of a loss of resilience (such as the disruption in daily activity patterns in cows after calving (van Dixhoorn et al. [2018])).

It may be argued that our method rests on the particular choice of the model given in equation (1). As we discuss in the appendix, equation (1) represents the simplest, albeit non-trivial representative of a broader family of synchronization dynamics. Different choices yield different geometries in the bifurcation diagram (figure 1, first row), but the main characteristic, the fact that at least one saddle-node bifurcation exists, remains true. This, together with the method to extract phase differences for general time series of periodically forced systems, makes our approach valid under very general circumstances. Two

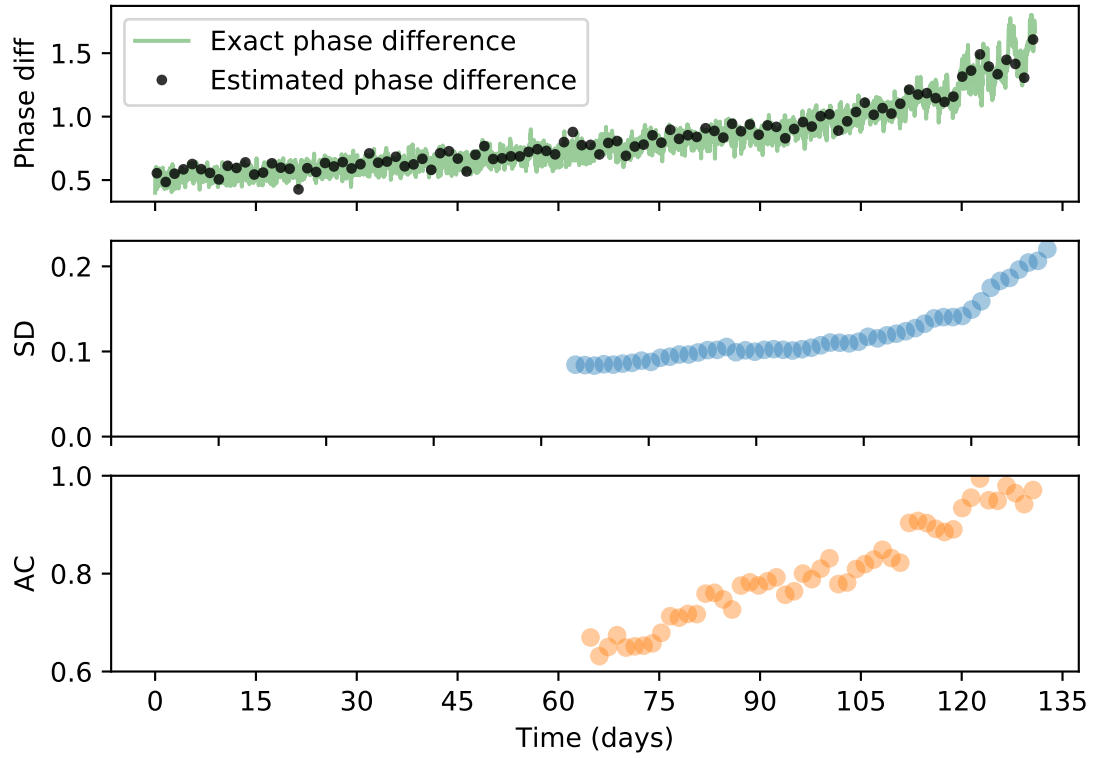


Figure 5: The black dots in the upper panel represent the phase difference, as approximated by our method. The exact phase difference is also shown (green line) as a reference of the method's accuracy. The central and lower panel show the standard deviation (in blue) and the autocorrelation with a 24 h lag (in orange) of the estimated phase difference, both of them calculated for a window 50% the length of the data. In both panels, as the time increases, the resilience of our system gets weaker.

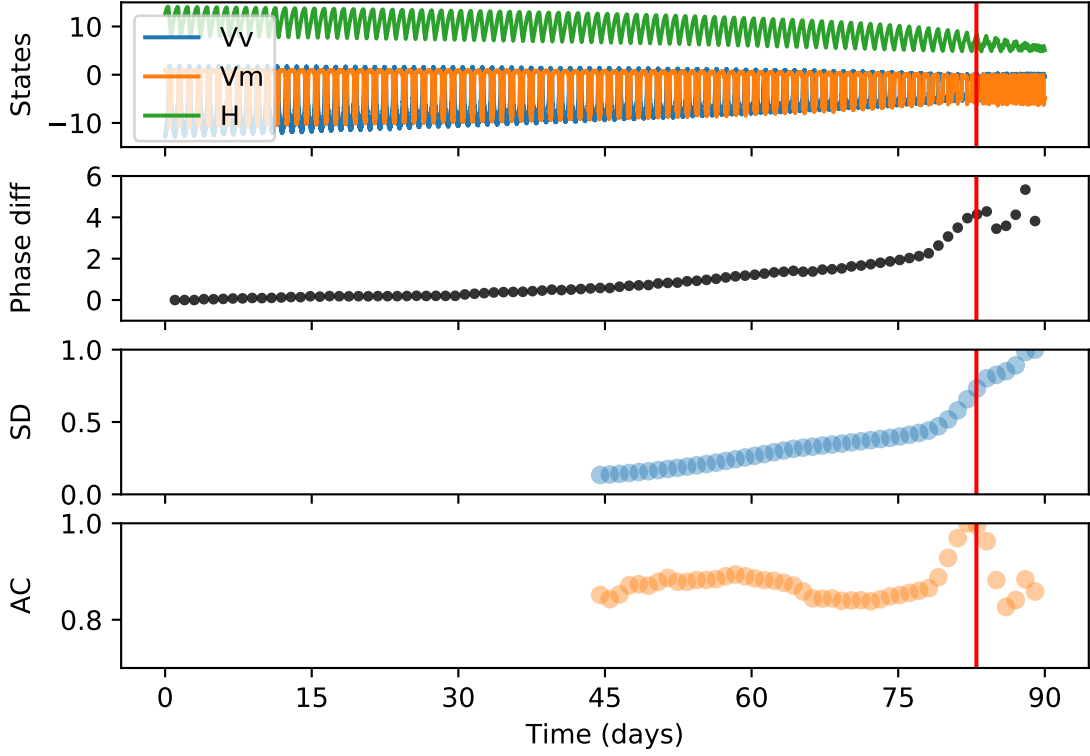


Figure 6: The upper panel shows a simulated time series obtained by integrating the Phillips-Robinson model under the influence of stochastic noise, and with the parameter ν_{vc} decreasing linearly in time to simulate an increasing difficulty in synchronizing. The simulation was initialized with non-transient values, to ensure the first days represent a healthy sleep wake cycle. The second panel shows the estimated phase difference (in hours) using the method described in our paper (sub-sampling the whole time series once per day, and using day 1 as reference). Our reference time series was chosen to be the somnogen level H during the first day. The two lower panels show the standard deviation (in blue) and the autocorrelation with a 48 h lag (in orange), calculated for a window of 45 days into the past, of the estimated phase differences. The red line the 83rd day marks the first episode of insomnia/desynchronization.

application examples of time series that were generated with two different sleep-wake models, Strogatz’s and Phillips-Robinson’s are analyzed.

The method to extract phase differences requires an approximate reference time series. In the Strogatz’s model application example we used the very simple assumption that a healthy individual sleeps from 0 h at night to 8 h in the morning. Some problems may benefit from or even require more sophisticated assumptions. In the absence of any detailed knowledge of the system under study, another approach could be using the dynamics of an arbitrary day as a reference. This is what we did in the Phillips-Robinson application example.

Additionally, our method requires high quality time series. Those time series should be long (as we need many cycles to infer the indicators) and should have a high density of data points (typically of the order of 10 points measured per cycle, depending on the shape of the time series). This makes our method less suitable to be applied with success in fields where the data is difficult and/or expensive to collect. Luckily, data-rich systems such as the ones provided by wearable devices are becoming increasingly popular in medicine or veterinary sciences.

Even after extracting the phase difference, the critical slowing down may be difficult to detect under some circumstances. As already noted in Dakos et al. [2015], his method to forecast saddle-node bifurcations has some fundamental limitations. For instance, it is required that the time-scale of the changes in the external forcing to be slower than the natural time-scale of the system (that is, the transitions shouldn’t be too sudden). The role of noise is also a delicate issue. On one hand, noise is required in order to observe the phenomenon of critical slowing down in the vicinity of a saddle-node bifurcation. On the other hand, it obscures the deterministic dynamics. Our analysis will prove weak for systems whose dynamics are strongly dominated by noise. Our method, based on Dakos’ indicators, shares this set of limitations.

Even with those applicability challenges, we consider our method to be a step in the direction of forecasting transitions between synchronized and desynchronized states. The fact that the disruption in certain physiological rhythms is associated with disease (Glass [2001]), together with the recent increase in the availability of high-quality biometric time series, makes the analysis and potential forecasting of these relevant kind of transitions a topic worth being explored.

5 Acknowledgments

We thank Ingrid van Dixhoorn and Rudi de Mol for their useful comments and suggestions.

This work was supported by funding from the European Union’s *Horizon 2020* research and innovation programme for the *ITN CRITICS* under Grant Agreement Number 643073.

Appendix

A.1 Detailed derivation of the phase extracting method

In order to justify the results of section 2.2, we will make use of equations (1), (4), (5) and (6). As a first step, we will write both sides of equation (6) in terms of M . We can do this by directly applying (4) and (5). The result is shown in equation (A.1).

$$\begin{cases} y(t) &= M[\theta(t)] \\ y^{ref}(t + \lambda) &= M[\theta_{\odot}(t + \lambda)] \end{cases} \quad (\text{A.1})$$

In order to be able to compare the functions given by equations (4) and (5) we will change their coordinates. Using the phase difference ($\phi(t) \equiv \theta(t) - \theta_{\odot}(t)$), we can rewrite the equation (4) in terms of θ_{\odot} and ϕ (see first line in equation (A.2)). Introducing a leftwards shift λ in the time coordinate of equation (5) it takes the form $y^{ref}(t + \lambda) = M[\theta_{\odot}(t + \lambda)]$, where $\theta_{\odot}(t + \lambda)$ can be evaluated exactly by its first order Taylor expansion, that is, $\theta_{\odot}(t + \lambda) = \theta_{\odot}(t) + \omega_{\odot}\lambda$ (cf. second line of equation (1)). The results of both coordinate transformations appear in equation (A.2).

$$\begin{cases} y(t) &= M[\theta_{\odot}(t) + \phi(t)] \\ y^{ref}(t + \lambda) &= M[\theta_{\odot}(t) + \omega_{\odot}\lambda] \end{cases} \quad (\text{A.2})$$

Note that if the system is synchronized and/or if the adiabatic approximation (that is, that the external conditions vary slowly) holds in our region of interest ($t \in [t_a, t_b]$), $\phi(t)$ can be approximated by a constant ϕ . We can estimate the value of ϕ by finding the shift λ^{min} that minimizes the square distance between both functions (equation (A.3)). By direct inspection of equation (A.2) we see that this optimal value corresponds to a phase difference of $\phi = \omega_{\odot}\lambda^{min}$.

$$D^2(\lambda) = \int_{t_a}^{t_b} (y(s) - y^{ref}(s + \lambda))^2 ds \quad (\text{A.3})$$

When faced with experimental data, we'll have a collection of N measured values y_i sampled at times t_i (that is, $y_i = y(t_i)$). The discrete equivalent of equation (A.3), representing the square distance between our measured and the expected points, is given in (7). By finding the value of the time displacement λ that minimizes $D^2(\lambda)$, we find the time delay that better fits our data (see figure 3).

A.2 Further generalization

By manipulating the parameter Ω/k in an equation like (2) with any non trivial continuous function $f(\phi)$ we are sure of encountering at least one saddle-node bifurcation. Even more, the saddle-node is the only kind of bifurcation that may happen.

This can be proven graphically. As we discussed in the methods section, the coupling function f in the model given by equation (2) can be any non-constant, continuous, smooth and periodic function, not necessarily a sine. A function f satisfying these properties will have at least one local minimum and one local maximum per period. This is also true for the right-hand side of equation (2). The effect of the parameter Ω/k is to move up and down the curve defined by $y(\phi) = \Omega - kf(\phi)$, whose roots represent the equilibria. This rules out the pitchfork and the transcritical bifurcations, as those require a change in the shape of the curve $y(\phi)$ (Strogatz [2003]). By manipulating the parameter Ω/k , the only possible bifurcations are collisions of stable and unstable equilibria, that is, saddle-node bifurcations (Strogatz [2003]). Those bifurcations happen when a minimum or a maximum equals 0 (see figure A.1).

Those readers familiar with analysis may prefer noticing that, in the vicinity of a minimum/maximum (ϕ_0), the second order Taylor expansion of the right-hand side of equation (2) can be written as the equation of a parabola (A.4).

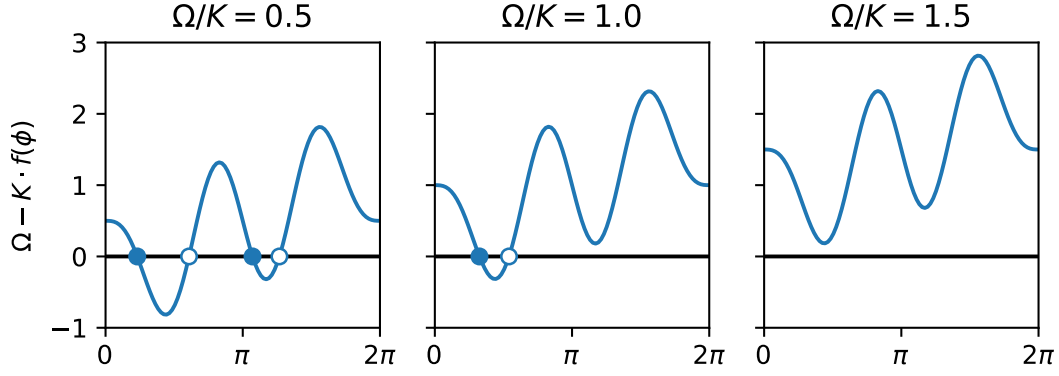


Figure A.1: Here we plot the curve $y(\phi) = \Omega - kf(\phi)$ for a non-sinusoidal coupling function f . The function is non-constant, continuous, smooth and periodic. We plotted it for three different values of the bifurcation parameter $\frac{\Omega}{k}$. The roots of each curve represent the equilibria (filled dots if stable, white if unstable).

$$\Omega - kf(\phi) \approx \Omega - kf(\phi_0) + \frac{kf''(\phi_0)}{2}(\phi - \phi_0)^2 \quad (\text{A.4})$$

By using the new variable $x \equiv \sqrt{\frac{kf''(\phi_0)}{2}}(\phi - \phi_0)$ (representing a shift and re-scale of the horizontal axis), and renaming $\Omega - kf(\phi_0)$ as r , the right-hand side of equation (A.4) adopts the canonical form of saddle-node bifurcation, i.e.: $r + x^2$ (Kuznetsov [1998]).

Due to the generality of the conditions requested to the coupling function f , we expect saddle-node bifurcations in the phase difference to be a widespread mechanism of synchronization and desynchronization. Consequently, we expect those bifurcations to be susceptible of being detected by the method described in this manuscript.

A.3 Parameters for Phillips-Robinson model

The parameters used in equation (8) are the same as in (Phillips and Robinson [2007]), with the exception of ν_{vc} , that decreases linearly from 6.3 mV to 0 mV along the period of 90 days. The time units have been changed to hours. The dynamics of the model are summarized in figure A.2. A usable implementation of this model (in R) can be found at <https://github.com/PabRod/sleepR>.

Symbol	Value	Units
τ_m	10/3600	h
τ_v	10/3600	h
χ	10.8	h
ν_{vm}	1.9/3600	$mV \cdot h$
ν_{mv}	1.9/3600	$mV \cdot h$
ν_{vh}	0.19	$mV \cdot nM^{-1}$
μ	10^{-3}	$nM \cdot h$
ν_{vc}	6.3 – 0	mV
$\nu_{ma}S(V_{a0})$	1	mV
Q_{max}	100 · 3600	h^{-1}
θ	10	mV
σ	3	mV
ω	$2\pi/24$	h^{-1}
α	0	1

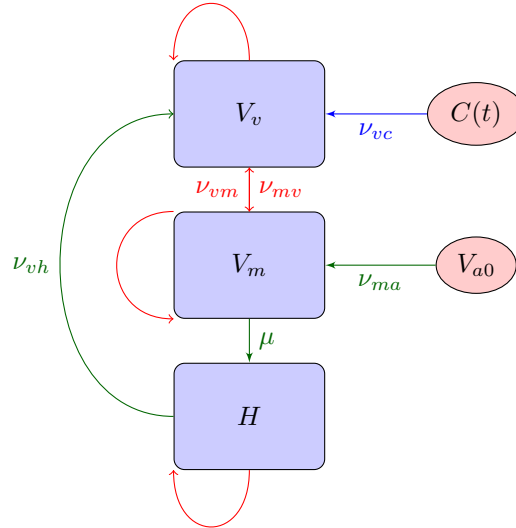


Figure A.2: Schematic summary of the dynamics of the Phillips-Robinson model. The light blue nodes represent the system's states (V_v the activity of the ventrolateral preoptic area, V_m the activity of the mono aminergic group and H the homeostatic pressure). The pink nodes represent the external sources ($C(t)$, the astronomical light/dark forcing, and V_{a0} , the acetylcholine group constant influence). The positive effects are coded as green arrows. Negative ones as red arrows. Blue arrows represent oscillating effects.

References

- Vasilis Dakos, Stephen R Carpenter, William A Brock, Aaron M Ellison, Vishwesha Guttal, Anthony R Ives, Sonia Kéfi, Valerie Livina, David A Seekell, Egbert H van Nes, and Marten Scheffer. Methods for detecting early warnings of critical transitions in time series illustrated using simulated ecological data. *PloS one*, 7(7):e41010, jan 2012. ISSN 1932-6203. doi: 10.1371/journal.pone.0041010. URL <http://journals.plos.org/plosone/article?id=10.1371/journal.pone.0041010>.
- Vasilis Dakos, Stephen R. Carpenter, Egbert H. van Nes, and Maórten Scheffer. Resilience indicators: Prospects and limitations for early warnings of regime shifts. *Philosophical Transactions of the Royal Society B: Biological Sciences*, 370(1659):1–10, jan 2015. ISSN 14712970. doi: 10.1098/rstb.2013.0263.
- Jean-Jacques d’Ortous de Mairan. Observation botanique. *Histoire de l’Academie Royale des Sciences*, 31:35–36, 1729.
- Russell G. Foster and Leon Kreitzman. *Circadian rhythms. A very short introduction*. Oxford University Press, 2017. ISBN 9780198717683.
- Leon Glass. Synchronization and rhythmic processes in physiology. *Nature*, 410(6825):277–284, mar 2001. ISSN 0028-0836. doi: 10.1038/35065745. URL <http://www.nature.com/doifinder/10.1038/35065745>.
- Yoshiki Kuramoto. Self-entrainment of a population of coupled non-linear oscillators. In *International Symposium on Mathematical Problems in Theoretical Physics*, pages 420–422. 1975.
- Yuri A. Kuznetsov. Elements of Applied Bifurcation Theory, Second Edition. *Library*, 1998. ISSN 0066-5452. doi: 10.1007/b98848.
- A.J.K. Phillips and P.A. Robinson. A Quantitative Model of Sleep-Wake Dynamics Based on the Physiology of the Brainstem Ascending Arousal System. *Journal of Biological Rhythms*, 22(2):167–179, apr 2007. ISSN 0748-7304. doi: 10.1177/0748730406297512. URL <http://journals.sagepub.com/doi/10.1177/0748730406297512>.
- Marten Scheffer. *Critical Transitions in Nature and Society*. 2009. ISBN 9780691122038. doi: 10.5860/CHOICE.47-1380. URL <http://books.google.com/books?id=jYSZgaaxRv0C>.

- Marten Scheffer, Jordi Bascompte, William a Brock, Victor Brovkin, Stephen R Carpenter, Vasilis Dakos, Hermann Held, Egbert H van Nes, Max Rietkerk, and George Sugihara. Early-warning signals for critical transitions. *Nature*, 461(7260):53–59, 2009. ISSN 0028-0836. doi: 10.1038/nature08227. URL <http://dx.doi.org/10.1038/nature08227>.
- Steven H. Strogatz. Human sleep and circadian rhythms: a simple model based on two coupled oscillators. *Journal of Mathematical Biology*, 25(3):327–347, jul 1987. ISSN 0303-6812. doi: 10.1007/BF00276440. URL <http://link.springer.com/10.1007/BF00276440>.
- Steven H Strogatz. *Nonlinear Dynamics And Chaos: With Applications To Physics, Biology, Chemistry And Engineering*. 1994. ISBN 9788187169857.
- Steven H. Strogatz. From Kuramoto to Crawford: exploring the onset of synchronization in populations of coupled oscillators. *Physica D: Nonlinear Phenomena*, 143(1):1–20, 2000. ISSN 01672789. doi: 10.1016/S0167-2789(00)00094-4. URL [https://doi.org/10.1016/S0167-2789\(00\)00094-4](https://doi.org/10.1016/S0167-2789(00)00094-4).
- Steven H Strogatz. *SYNC: The Emerging Science of Spontaneous Order*. Penguin Books, 2003. ISBN 978-0-14-100763-2.
- I.D.E. van Dixhoorn, R.M. de Mol, J.T.N. van der Werf, S. van Mourik, and C.G. van Reenen. Indicators of resilience during the transition period in dairy cows: A case study. *Journal of Dairy Science*, 101(11):10271–10282, nov 2018. ISSN 0022-0302. doi: 10.3168/JDS.2018-14779. URL <https://www.sciencedirect.com/science/article/pii/S0022030218308701?via%3Dihub>.
- Egbert H. Van Nes and Marten Scheffer. Slow recovery from perturbations as a generic indicator of a nearby catastrophic shift. *American Naturalist*, 169(6):738–747, jun 2007. ISSN 00030147. doi: 10.1086/516845.
- C. Wissel. A universal law of the characteristic return time near thresholds. *Oecologia*, 65(1):101–107, dec 1984. ISSN 00298549. doi: 10.1007/BF00384470.